RESEARCH ARTICLE

Semi-Parametric Control Architecture for Autonomous Underwater Vehicles Subject to Time Delays

IGNACIO CARLUCHO[1,2], **(Member, IEEE), DYLAN STEPHENS**[1], **WILLIAM ARD**[1], **AND CORINA BARBALATA**[1]

[1]Department of Mechanical and Industrial Engineering, Louisiana State University, Baton Rouge, LA 70803, USA
[2]School of Engineering and Physical Sciences, Heriot-Watt University, EH14 4AS Edinburgh, U.K.

Corresponding author: Corina Barbalata (cbarbalata@lsu.edu)

ABSTRACT This paper presents a data-driven model-based control system for autonomous underwater vehicles (or AUVs) subject to input delays. This work is motivated by the input time delays that can arise in underwater robotics due to communication restrictions and sensor malfunctions. Such delays can highly degrade the performance of classical control structures resulting in unpredictable system behaviours. The proposed control architecture addresses such limitations. The approach incorporates a linear dynamic representation of the system obtained using the Koopman operator in an observer/state prediction formulation. The proposed control architecture is designed based on discrepancies between the data-driven estimation of the system's behaviour and the actual AUV performance using chain predictors. The capabilities of the proposed approach are shown through experiments performed with a 4 degrees-of-freedom autonomous underwater vehicle. The results demonstrate stable behaviours without steady-state errors, even in the presence of long delay.

INDEX TERMS Autonomous underwater vehicles, control theory, Koopman operator, model based control, observer-based predictors.

I. INTRODUCTION

Underwater robotic systems have become popular in the last decade due to their ability to explore difficult and uncharted territories. Remotely operated vehicles (or ROVs) and AUVs have been used in military applications [1], oil and gas applications [2], and scientific research [3]. ROVs require expert knowledge to control the system but they can spend extended periods of time in the water performing exploration work. AUVs can spend a limited amount of time exploring the environment, but they have the benefit of being autonomous and can easily reach confined spaces. As for any modern system, ROVs and AUVs require reliable control systems that can ensure robust behaviour regardless of the operating conditions. The design of control architectures for underwa-

ter robotic systems includes difficulties such as parametric uncertainties, nonlinearities in the dynamics of the system, sudden external disturbances [4], communication delays [5], or lagged information from the navigation sensors. Furthermore, there are cases when the control system has to handle input delays of unknown time [4], due to sensor failure, bandwidth limitations in communication, limited internal working frequency of on-board sensors, or discrepancies with the microcontroller requirements [6].

The research community has focused on designing control algorithms that address these challenges primarily based on the assumptions that either there are accurate mathematical models available, or that enough data about the system's behaviour can be obtained [7], [8]. A popular technique investigated by the control community is time delay compensation, where if the delay is sufficiently small, a control law based on the delayed dynamic model can be used to compensate

The associate editor coordinating the review of this manuscript and approving it for publication was Yilun Shang.
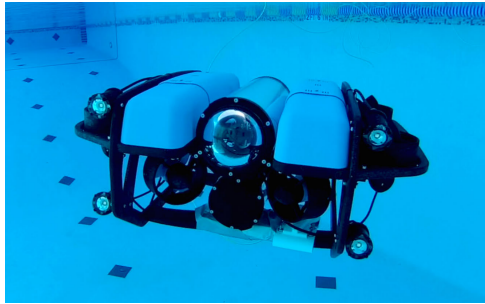
FIGURE 1. BlueROV2Heavy has been modified to enable fully autonomous capabilities.

for unknown disturbances and parameters in the dynamic model [9]. This approach consists of developing a feedback control loop that can compensate for delayed output measurements or state information and produces asymptotically stable behaviour. However, these types of approaches usually assume that the delay quantity is known in advance [10]. The method of sequential predictors [11] is part of a family of time delay techniques where the original model of the system is operated at different time scales, producing a dynamic extension whose state variable can be used in the feedback control in order to achieve the desired delay compensation. These methods ensure input-to-state stability with respect to uncertainties [12], while at the same time compensating for arbitrarily long delays [13]. They have been designed and investigated for nonlinear systems with bounded uncertainties and have been validated from a theoretical perspective. However, one drawback of the sequential predictor methods is that they require a perfect knowledge of the system dynamics [11].

Obtaining an accurate dynamic model for underwater vehicles can be time-consuming and challenging, as the system is highly nonlinear and unknown hydrodynamic effects are present [14]. These limitations have the potential to be addressed by leveraging modern machine learning approaches [15]. However, techniques such as neural networks provide a black-box type of approach that in some cases may not be directly applicable to classical control formulations. Nevertheless, one data-driven approach based on Koopman operators [16] has been introduced and studied in several papers focused on dynamic model estimation and model-based control [17], [18]. Koopman-based methods focus on the dynamical model of the system in an explicit control-oriented description without any simplifications regarding the behaviour of the system being modeled [19]. As such, Koopman modelling techniques achieve a semi-parametric model, where the model's structure maintains an equation-based representation, while the parameters are obtained through data. This opens a new avenue of research in which model-based control methodologies can be used in combination with Koopman operators to obtain a class of data-driven control systems [20].

In this work, we aim to leverage the advancements of dynamic modelling using Koopman operators to design a novel semi-parametric prediction control structure for coupled nonlinear systems with model uncertainties and unknown input delays. Specifically, we designed and developed a low-level control law for autonomous underwater vehicles, such as the one seen in Fig. 1, where communication delays between the top-side computer (responsible for the high-level decision making) and the microcontroller are present. The contributions of this work are as follows:

- The design of a novel prediction-based control law for high-dimensional nonlinear systems with large parametric uncertainties.
- The development of a data-driven model for a high-dimensional underwater system based on the Koopman operator.
- The experimental evaluation of time-delayed controllers for small-sized autonomous underwater vehicles.

The remainder of the paper is structured as follows. In Section II, we provide a summary of modelling and control methods for underwater marine vehicles and time delay control. In Section III, the problem to be solved is introduced, Section IV presents the modelling approach for marine vehicles. Section V describes the proposed control system. We detail our experimental results in Section VI where a discussion of the advantages and limitations of the control architecture is presented. Finally, the conclusions and future directions of this work are presented in Section VII.

II. RELATED WORK
Designing robust and reliable control systems for underwater robots is challenging due to nonlinearities, sudden and large environmental disturbances, high uncertainties in the hydrodynamic parameters, and time variation of the system. Such limitations are difficult to address by well-known linear controllers [21] and the research community has investigated strategies that perform well with nonlinear systems [22].

In [23], a fuzzy proportional integral derivative (PID) controller is presented for a spherical underwater robot. The controller computes the system error and its rate, leveraging this information to modify the gains of the PID controller based on fuzzy logic. The gains of proportional integral limited (or PLIM) controllers have been adapted online in [24] based on adaptive interaction theory. This approach compensates for any changes in the environmental characteristics or payload changes of the vehicle, addressing the challenge of uncertainty in the dynamic model of the system. This issue has also been investigated by using time delay control systems in [4] and [25]. For cases where time delay control systems are used, it has been shown that if the delay time is sufficiently small, then a control law based on the delayed dynamic model can be used to compensate for unknown disturbances and parameters in the dynamic model [9]. Furthermore, time delay control approaches are extremely attractive for the area of coordinated underwater vehicles

where leader-follower based approaches are used. The low data transmission of acoustic modems introduces communication delays in the control structure [26]. Approaches such as event-triggered control [27] or gradient descent delay estimators [26] have been used to control teams of AUVs with kinematic representations, without taking into account the dynamics of the system and the large uncertainties in the models. Nevertheless, for marine vehicles, where communication with other robotic systems or human operators is required, designing low-level control methods that consider the hydrodynamics are essential. Methods such as the one presented in [4] cannot guarantee robust behaviour if large delays due to communication constraints are present. Another method, used in the control of AUVs, is that of fixed-time controllers [28], however these do not take into consideration delays in the system [29], [30].

One delay compensation approach shown in literature uses sequential-predictor-based methods that can compensate for large delays [31]. The characteristic of such a controller is the use of predictors to define a variable that will replace the state of the system in the feedback formulation. This eliminates the effects of system delay [32]. In [31], the authors present a sequential predictor approach to compensate for both input and measurement delays. In [33], the authors introduce the idea of sequential structures for sub-predictors to control unstable systems with long time-delay. This approach designs coupled prediction models, with each being used to estimate the state on an interval that corresponds to a suitable fraction of the delay. A similar idea has been presented in [34] where the sub-predictors have been integrated with H_∞ control. In [13], a sequential predictor for discrete-time systems with time-varying delays is presented, where the number of the predictors is an upper bound for the delay.

The above mentioned methods are highly desirable as they can produce global asymptotic stabilisation of the system. The work done in the area of sequential predictors has focused on providing asymptotic convergence properties. However, the computational load and time of previously reported sequential-predictor control methods represents a limitation for their implementation on robots with limited computational capabilities and operational power. Another limitation of such control approaches is the assumption that the models used in the predictors are known except for their having an unknown additive uncertainty. This is not the case for underwater vehicles where physics-based methods such as the ones presented in [35] and [36] suffer from high uncertainties in the hydrodynamic parameters. An approach to address this limitation in the model is the use of data-driven approaches. In [37] a neurofuzzy model of an AUV is generated. However, the identification of the system requires initial expert knowledge, which is later refined by data-driven formulations. In [38], a long short-term memory (or LSTM) network is used to model the dynamics of an AUV. This model is later used to identify faults in the sensors of the vehicle by comparing the predicted behaviour with the actual

observed performance. A neural network model for an underwater arm was developed in [14], and used in combination with a model predictive controller (or MPC) for the efficient manipulation of unknown payloads.

While these data-driven methodologies provide ample modelling possibilities, they produce a black-box type model that may be difficult to integrate with existing control methodologies. Koopman operator theory presents an alternative procedure, as it is able to produce linear models of nonlinear systems directly from data [39]. In [19], Koopman operators together with an MPC are used for the control of a soft robotic arm. In [40], graph neural networks are used as basic functions for calculating Koopman operators. The states are encoded with the graph neural network into object-centric embeddings, achieving generalisation. However, while Koopman operators provide fast and simple models that can be readily integrated with classical control methods, their application to real-time robotics systems has been limited, with no works for underwater systems.

III. PROBLEM STATEMENT

Consider a nonlinear model of an underwater vehicle system of the form:

$$\dot{\mathbf{x}}(t) = F(\mathbf{x}(t), \mathbf{v}(t), \mathbf{u}(t - \tau)) \qquad (1)$$

where $\mathbf{x}$ is valued in $\mathbb{R}^q$ and represents the states of the marine robotic system, the piece-wise C^1 function $\mathbf{v}$ is valued in $\mathbb{R}^q$ and represents uncertainty, $\mathbf{u}$ is valued in $\mathbb{R}^m$ and represents the control inputs, and $\tau > 0$ is the unknown time delay. The objective of this paper is to specify the feedback control $\mathbf{u}$ such that for a desired reference trajectory $\mathbf{x}_{ref}$, the dynamics for $\mathbf{x} - \mathbf{x}_{ref}$ are globally asymptotically stable to the origin on $\mathbb{R}^q$.

An intermediate step in achieving this goal is to obtain a high-accuracy discrete linear representation of the physical system shown in Equation (1), which could be formulated as:

$$\mathbf{x}[k] = A\mathbf{x}[k] + B\mathbf{u}[k - \tau] + E\mathbf{v}[k] \qquad (2)$$

where $A \in \mathbb{R}^{q \times q}$, $B \in \mathbb{R}^{q \times m}$ and $E \in \mathbb{R}^{q \times q}$ are constant matrices, and $\tau > 0$ is a constant unknown discrete delay. Note that we abuse the notation here and utilise τ both for the continuous and discrete representation, this allows us to keep a consistent notation. Unlike non-linear methods, linear models are easier to compute, providing faster and simpler implementations. This is desired in mobile robots where on-board computer capabilities are limited, especially in the underwater domain.

Remark 1: Due to the constant unknown input delay τ, defining solutions of Equation (1) calls for initial functions of $\mathbf{x}$ that are defined in $[t_0 - \tau, \ t_0]$ and valued in $\mathbb{R}^q$ (instead of using initial states $\mathbf{x}_0 \in \mathbb{R}^q$, which would be called for when no delays were present), where t_0 is the initial time for the solution. Letting $|\cdot|$ denote the usual Euclidean norm, our assumption is as follows:

Assumption 1: There is an unknown constant $\Omega > 0$ such that $|\mathbf{v}(t)| < \Omega$ for all $t \geq 0$.

IV. SEMI-PARAMETRIC DYNAMIC MODELLING

A. NONLINEAR DYNAMIC REPRESENTATION

In this subsection, we specify a nonlinear representation of an AUV with uncertainties caused by unknown hydrodynamic parameters and environmental disturbances, and with input time delays. The vehicle's pose in the world coordinate frame is represented by $\boldsymbol{\eta}(t) = [x_l(t), y_l(t), z_l(t), \phi_a(t), \theta_a(t), \psi_a(t)]^T$, at time t, with $x_l(t)$, $y_l(t)$ and $z_l(t)$ being the position in the x, y and z plane respectively, $\phi_a(t)$ being the roll, $\theta_a(t)$ being the pitch, and $\psi_a(t)$ being the yaw of the vehicle. Additionally, the vehicle's body-fixed velocity vector is represented by $\boldsymbol{v}(t) = [u(t), v(t), w(t), p(t), q(t), r(t)]^T$. The time delay control inputs are represented by $\mathbf{u}(t - \tau)$. The dynamics of the AUV can be expressed as:

$$\begin{cases} \dot{\boldsymbol{\eta}}(t) = R_B^I \boldsymbol{v}(t) \\ \widetilde{M} \dot{\boldsymbol{v}}(t) + \widetilde{C} \boldsymbol{v}(t) + \widetilde{D} \boldsymbol{v}(t) + \widetilde{\mathbf{g}} = \mathbf{u}(t - \tau) + \mathbf{v}(t) \end{cases} \quad (3)$$

where R_B^I is the rotation matrix from the body frame to the inertial frame, $\widetilde{M}$ is an estimate of the inertia matrix, $\widetilde{C}$ contains the estimated Coriolis and centrifugal terms, $\widetilde{D}$ contains the estimated hydrodynamic damping terms, and $\widetilde{\mathbf{g}}$ are the estimated restoring forces. The requirements for Equation (3) are those given in Section III. Particularly that, $\tau > 0$ and Assumption 1 must hold true.

The dynamics of the AUV presented in Equation (3) can also be expressed in a general way as in Equation (1), where the state of the system $\mathbf{x}(t)$ can be defined as $\mathbf{x}(t) = [\boldsymbol{\eta}(t), \boldsymbol{v}(t)]$. Since it is difficult to estimate the dynamic parameters in Equation (3) due to different water conditions and challenges in hydrodynamics estimation [30], semi-parametric modelling approaches can be more suitable. In this paper, we propose to use a Koopman operator [41] for the modelling of underwater vehicles.

B. LINEARISED DYNAMICS USING KOOPMAN OPERATOR

For a nonlinear system of the form:

$$\dot{\mathbf{x}}(t) = F(\mathbf{x}(t), \mathbf{u}(t)) \quad (4)$$

predicting the behaviour of the system at time t given the initial state $\mathbf{x}_0$ and a set of values $\{\mathbf{u}_0, \mathbf{u}_1, \ldots, \mathbf{u}_t\}$ for the control inputs in $\mathbb{R}^m$ can be done using Koopman operators. To achieve this, the system in Equation (4) can be lifted to an infinite dimensional function space $\mathcal{F}$, in which the flow of the system is described based on a Koopman operator, which is a collection of functions $\mathcal{K}_t : \mathcal{F} \to \mathcal{F}$ for $t \geq 0$ [42]. The elements $f \in \mathcal{F}$ are called observables and the evolution of the system can be described as:

$$\mathcal{K}_t f = f \circ \phi_t \quad (5)$$

where $\circ$ is the composition operator, and the flow map ϕ_t of Equation (4) is defined such that $\phi_t(\mathbf{x}_0)$ is the solution of Equation (4) at each time $t \geq t_0$ for each given initial state $\mathbf{x}_0$, and for a given fixed initial time $t_0 \geq 0$.

This operator fully captures the properties of the underlying system, providing a linear representation of the nonlinear system in the infinite-dimensional space of observables. However, it is not possible to express the Koopman operator as a finite-dimensional matrix, since $\mathcal{F}$ is infinite-dimensional, but it is possible to project the Koopman operator to a finite-dimensional subspace and represent it as a matrix [19]. Therefore, we are interested in finding a finite dimensional representation of the Koopman operator. Usually, this representation is learned by data using a set of $P \in \mathbb{N}$ measurements [42]. To achieve this, the extended dynamic mode decomposition (or EDMD) algorithm [16] has been previously used in various applications [43], [44] and will be employed in this paper.

We start by defining a subspace $\bar{\mathcal{F}} \subset \mathcal{F}$ spanned by a basis of linearly real valued independent functions ψ_i, where $i = 1, \ldots, N$, and a vector valued function $\psi(\mathbf{x}) = [\psi_1(\mathbf{x}), \psi_2(\mathbf{x}), \cdots, \psi_N(\mathbf{x})]$, where $\mathbf{x} = [x_1, \ldots, x_q]^T$. Then using a set of experimental data $(\mathbf{x}[k], \mathbf{x}[k + 1])$ for each $k \in 1, \ldots, P$, we construct a series of snapshot pairs:

$$\boldsymbol{\alpha}[k] = \begin{bmatrix} \psi(\mathbf{x}[k]) \\ \mathbf{u}[k] \end{bmatrix} \quad \text{and} \quad \boldsymbol{\beta}[k] = \begin{bmatrix} \psi(\mathbf{x}[k + 1]) \\ \mathbf{u}[k] \end{bmatrix}$$

where $\mathbf{x}[k]$ and $\mathbf{u}[k]$ are the state vector and the control value used in the dynamics represented by Equation (4) at each of the discrete times k.

These consecutive snapshot pairs do not have to be generated by consecutive state measurements. Note that we also include the non-lifted input $\mathbf{u}[k]$ in the snapshot, which will allow us to combine this method with feedback control design.

The problem is now focused on finding a data-based approximation U of the Koopman operator, from a set of data points by solving the optimisation problem in Equation (6). This is obtained based on the EDMD algorithm presented in [45].

$$\min_U \sum_{t=1}^{P} |U^T \boldsymbol{\alpha}[k] - \boldsymbol{\beta}[k]|^2 \quad (6)$$

We assume that U is build based on $A \in \mathbb{R}^{N \times N}$ and $B \in \mathbb{R}^{N \times m}$, such that:

$$U^T = \begin{bmatrix} A & B \\ O & I \end{bmatrix} \quad (7)$$

where O and I and the zero and identity matrices of the required dimensions. The problem of finding the optimal U from a set of data points can then be reformulated as:

$$\min_{A,B} \sum_{t=1}^{P} |A\psi(\mathbf{x}[k]) + B\mathbf{u}[k] - \psi(\mathbf{x}[k + 1])|^2 \quad (8)$$

This last expression allows us to obtain the A and B parameters from data for discrete-time systems. The Koopman representation can be expressed as:

$$\bar{\mathbf{x}}[k + 1] = A\bar{\mathbf{x}}[k] + B\mathbf{u}[k] \quad (9)$$

where $\bar{\mathbf{x}}[k] = \psi(\mathbf{x}[k])$. In the following section, we will utilise this representation to define an observer-based control system for AUV under variable time delays.

V. CONTROLLER DESIGN

In this section, we present the derivation of the proposed control architecture for systems with input time delay. The proposed approach leverages the Koopman estimation for state observer formulations within a cascaded feedback architecture.

Using the Koopman operator as presented in Section IV-B, the linearised representation of the AUV with input delays is given by:

$$\bar{\mathbf{x}}[k+1] = A\bar{\mathbf{x}}[k] + B\mathbf{u}[k-\tau]$$
$$\mathbf{y}[k] = C_c\bar{\mathbf{x}}[k] \qquad (10)$$

where the lifted state vector $\bar{\mathbf{x}} = \psi(\mathbf{x})$ is valued in $\mathbb{R}^N$, the control input vector $\mathbf{u}$ is valued in $\mathbb{R}^m$, the observation vector $\mathbf{y}$ is valued in $\mathbb{R}^q$, $C_c \in \mathbb{R}^{q\times N}$, and τ denotes some constant unknown time delay.

Assumption 2: (A, B) is controllable, and $\mathbf{y}[k]$ is available for measurement.

Assumption 3: (A, C_c) is observable.

While Equation (10) models the dynamics of the system by utilising data gathered in various conditions, it is still necessary to account for discrepancies in the model caused by cases for which data is not available (i.e., impossible to obtain data for every single underwater condition where currents differ from region to region). To take these differences into consideration, it is possible to include a function in the Koopman formulation that represents these discrepancies to obtain:

$$\bar{\mathbf{x}}[k+1] = A\bar{\mathbf{x}}[k] + B\mathbf{u}[k-\tau] + E\mathbf{v}[k]$$
$$\mathbf{y}[k] = C_c\bar{\mathbf{x}}[k] \qquad (11)$$

with $E \in \mathbb{R}^{N\times q}$, and $\mathbf{v}[k]$ is unknown. In Section V-A, this representation is leveraged to obtain an observer structure, which allows for the construction of a control signal $\mathbf{u}$ that realises the objectives. This control signal is presented in Section V-B.

A. OBSERVER/STATE PREDICTION FORMULATION

Well known standard feedback laws will be able to stabilize the system when $\tau = 0$ in Equation (11), but will have limited application when $\tau > 0$. In a system with input delay as that of Equation (11), we are interested in obtaining an asymptotic state prediction based on a state observer [46]. The proposed approach is based on a class of observers, called sequential predictors, which provide an asymptotic estimation but require a model representation of the system. This paper presents the integration of the semi-parametric model based on the Koopman operator, obtained in Section IV-B, and the lifted representation of the state $\bar{\mathbf{x}}[k]$ in the sequential predictor formulation. Furthermore, it expands the standard sequential-predictor

formulation by integrating a proportional integral (PI) architecture into the formulation of sequential predictors.

Given the lifted estimation $\bar{\mathbf{x}}[k+\tau]$ at time $[k+\tau]$, and assuming $\bar{\mathbf{x}}[k]$ is known at time k, a proportional integral (or PI) observer-like structure [47] is designed based on:

$$\mathbf{z}[k+1] = A\mathbf{z}[k] + B\mathbf{u}[k]$$
$$\qquad - K\,(C_c\mathbf{z}[k-\tau] - \mathbf{y}[k]) + E\mathbf{d}[k]$$
$$\mathbf{d}[k+1] = \mathbf{d}[k] - L(C_c\mathbf{z}[t-\tau] - \mathbf{y}[k]) \qquad (12)$$

where $\mathbf{z}[k]$ is the estimate of $\bar{\mathbf{x}}[k+\tau]$, $\mathbf{d}$ is the estimation of the discrepancy between observations and predictions and is valued in $\mathbb{R}^q$, and $E \in \mathbb{R}^{N\times q}$, $K \in \mathbb{R}^{N\times q}$ and $L \in \mathbb{R}^{q\times q}$ are the gain matrices of the PI observer.

It is possible to define a new set of variables $\mathbf{w}[k] = [\mathbf{z}[k], \mathbf{d}[k]]^T$ and $\mathbf{x}_e[k] = [\bar{\mathbf{x}}[k], \mathbf{v}[k]]^T$ [48], which allows the reformulation of Equation (12) in compact form:

$$\mathbf{w}[k+1] = A_e\mathbf{w}[k] + B_e\mathbf{u}[k] - K_eC_e\,(\mathbf{w}[k-\tau] - \mathbf{x}_e[k]) \qquad (13)$$

where:

$$A_e = \begin{bmatrix} A & E \\ 0 & I \end{bmatrix},\ K_e = \begin{bmatrix} K \\ L \end{bmatrix},\ B_e = \begin{bmatrix} B \\ 0 \end{bmatrix},\ \text{and}\ C_e = \begin{bmatrix} C_c & 0 \end{bmatrix}$$

Now, the objective is to make the estimation error asymptotically decay to zero. The estimation error is defined as:

$$\mathbf{e}[k] = \begin{bmatrix} \mathbf{z}[k] - \bar{\mathbf{x}}[k+\tau] \\ \mathbf{d}[k] - \mathbf{v}[k+\tau] \end{bmatrix} = \mathbf{w}[k] - \mathbf{x}_e[k+\tau] \qquad (14)$$

and the error dynamics can be written as:

$$\mathbf{e}[k+1] = \mathbf{w}[k+1] - \mathbf{x}_e[k+1+\tau] \qquad (15)$$

with $\mathbf{w}[k+1]$ as in Equation (13). For simplicity, we assume that $\mathbf{v}$ is constant in what follows, but generalizations for nonconstant can be done using input-to-state stability [12]. Furthermore, $\mathbf{x}_e[k+1+\tau]$ can be written as:

$$\mathbf{x}_e[k+1+\tau] = A_e\mathbf{x}_e[k+\tau] + B_e\mathbf{u}[k] \qquad (16)$$

Combining $\mathbf{w}[k+1]$ and $\mathbf{x}_e[k+1+\tau]$ results in

$$\mathbf{e}[k+1] = A_e\mathbf{w}[k] + B_e\mathbf{u}[k] - K_eC_e(\mathbf{w}[k-\tau]$$
$$\qquad - \mathbf{x}_e[k]) - \mathbf{x}_e[k+1+\tau] \qquad (17)$$

which after simplifications yields:

$$\mathbf{e}[k+1] = A_e(\mathbf{w}[k] - \mathbf{x}_e[k+\tau]) - K_eC_e\,(\mathbf{w}[k-\tau] - \mathbf{x}_e[k]) \qquad (18)$$

Recalling that $\mathbf{e}[k] = \mathbf{w}[k] - \mathbf{x}_e[k+\tau]$, it can be introduced in Equation (18), which gives the equation of error dynamics of the form:

$$\mathbf{e}[k+1] = A_e\mathbf{e}[k] - K_eC_e\mathbf{e}[k-\tau] \qquad (19)$$

By properly choosing the gain matrices $K_e \in \mathbb{R}^{(N+q)\times q}$, we can ensure that Equation (19) is globally exponentially stable to 0 when $\tau > 0$ is small enough [49]. However, in this work, we are interested in obtaining a set of n partial-state

predictors-observers where n is the number of predictors. Therefore, following [32], Equation (13) can now be reformulated as:

$$\begin{aligned}
\mathbf{w}_1[k+1] &= A_e \mathbf{w}_1[k] + B_e \mathbf{u}[k - \tfrac{n-1}{n}\tau] \\
&\quad - K_{e_1} C_e (\mathbf{w}_1[k - \tfrac{\tau}{n}] - \mathbf{x}_e[k]) \\
\mathbf{w}_i[k+1] &= A_e \mathbf{w}_i[k] + B_e \mathbf{u}[k - \tfrac{n-i}{n}\tau] \\
&\quad - K_{e_i} C_e \left(\mathbf{w}_i[k - \tfrac{\tau}{n}] - \mathbf{w}_{i-1}[k] \right) \\
&\quad \text{for } 2 \le i \le n
\end{aligned} \tag{20}$$

Each $\mathbf{w}_i[k]$ is a prediction of $\mathbf{x}_e[k + i\tfrac{\tau}{n}]$. This will result in $\mathbf{w}_n[k] = [\mathbf{z}_n[k], \, \mathbf{d}_n[k]]^T$ being the last predictor and the most accurate estimator of the states of the system, if each K_{e_i} is chosen properly. Furthermore, each K_{e_i} and n will need to satisfy that: 1) $A_e - K_{e_i} C_e$ is Hurwitz and 2) n is large enough. The corresponding prediction error for each subsystem is:

$$\mathbf{e}_i[k] = \mathbf{w}_i[k] - \mathbf{x}_e\left[k + i\frac{\tau}{n}\right] \tag{21}$$

From Equation (20), and similarly as in [32], the error dynamics satisfy:

$$\mathbf{e}_i[k+1] = \mathbf{w}_i[k+1] - \mathbf{x}_e\left[k + 1 + i\frac{\tau}{n}\right] \tag{22}$$

Replacing Equation (20) in Equation (22) yields:

$$\begin{aligned}
\mathbf{e}_i[k+1] &= A_e \mathbf{w}_i[k] + B_e \mathbf{u}[k - \tfrac{n-i}{n}\tau] \\
&\quad - K_{e_i} C_e \left(\mathbf{w}_i[k - \tfrac{\tau}{n}] - \mathbf{w}_{i-1}[k] \right) \\
&\quad - \mathbf{x}_e\left[k + 1 + i\frac{\tau}{n}\right]
\end{aligned} \tag{23}$$

and knowing that $\mathbf{x}_e[k + 1 + i\tfrac{\tau}{n}] = A_e \mathbf{x}_e[k + i\tfrac{\tau}{n}] + B_e \mathbf{u}[k - \tfrac{n-i}{n}\tau]$, we can replace into Equation (23) and obtain:

$$\mathbf{e}_i[k+1] = A_e \mathbf{e}_i[k] - K_{e_i} C_e \mathbf{e}_i\left[k - \frac{\tau}{n}\right]$$
$$\text{with} \quad i \ge 1, \; \mathbf{e}_0 = 0 \tag{24}$$

B. FEEDBACK CONTROL FORMULATION

With the PI observer defined in the previous section, we now focus on designing a feedback control law $\mathbf{u}[k]$ that can stabilize the system presented in Equation (3) when $\tau > 0$. This $\mathbf{u}[k]$ is used in the observer predictor formulation in Section V-A. The current system's state, $\mathbf{x}[k] = [\boldsymbol{\eta}[k], \, \boldsymbol{v}[k]]^T$, is obtained on-line from the sensor readings on board of the AUV. A cascaded feedback formulation similar to the one presented in [50] is chosen due to its simplicity and effectiveness. The proposed cascade controller allows us to accurately compensate for changes in velocity, which occur rapidly, while at the same time reducing errors in the position [51]. Additionally, this architecture allows the selection of the system's operational mode to be able to switch between position control and velocity control [24]. The proposed architecture thus has two control loops, an outer proportional derivative (or PD) structure for position control, and an inner proportional integral derivative (or PID) controller for velocity regulation.

To control the system when $\tau > 0$, the asymptotic state prediction $\mathbf{z}_n[k]$, that is a component based of $\mathbf{w}_n[k]$, as defined in Section V-A, can now be utilized in the control formulation to obtain a control law that minimizes the error between the reference and the predicted state of the system. With the notation $\mathbf{y}_n[k] = C_c \mathbf{z}_n[k]$, and $\mathbf{y}_n[k] = [\mathbf{y}_n^p[k], \, \mathbf{y}_n^v[k]]^T$, we can then obtain Equation (25).

$$\mathbf{e}^p[k] = \mathbf{x}_{ref}^p[k] - \mathbf{y}_n^p[k]$$

$$\mathbf{e}^v[k] = \mathbf{u}^b[k] - \mathbf{y}_n^v[k]$$

$$\mathbf{u}^w[k] = \mathbf{u}^w[k-1] + \left(K_p^p + \frac{K_d^p}{\Delta t} \right) \mathbf{e}^p[k]$$
$$+ \left(-K_p^p - \frac{2K_d^p}{\Delta t} \right) \mathbf{e}^p[k-1] + \frac{K_d^p}{\Delta t} \mathbf{e}^p[k-2]$$

$$\mathbf{u}[k] = \mathbf{u}[k-1] + \left(K_p^v + K_i^v \Delta t + \frac{K_d^v}{\Delta t} \right) \mathbf{e}^v[k]$$
$$+ \left(-K_p^v - \frac{2K_d^v}{\Delta t} \right) \mathbf{e}^v[k-1] + \frac{K_d^v}{\Delta t} \mathbf{e}^v[k-2] \tag{25}$$

where Δt is the sampling period, $\mathbf{e}^p$ is the error in position, $\mathbf{e}^v$ is the error in velocity, $\mathbf{u}^w$ is the quasi-velocity generated by the outer control loop, K_p^p and K_d^p are the proportional and derivative gains of the outer loop and K_p^v, K_d^v and K_i^v are the proportional, derivative and integral gains of the inner PID. The outer control loop utilizes a PD controller and it takes as input the error $\mathbf{e}^p$ calculated as the difference between the desired AUV pose, $\mathbf{x}_{ref}^p(t)$, and the estimated AUV pose, $\mathbf{y}_n^p(t)$, expressed in the world coordinates. The output of the outer PD controller, $\mathbf{u}^w$, is transformed into the body frame, utilizing the rotation matrix R_B^I, and provides the quasi-velocity reference to the inner control loop, such that $\mathbf{u}^b(t) = R_B^I \mathbf{u}^w(t)$. The inner structure takes as input the error $\mathbf{e}^v(t)$, and gives as output the feedback control law $\mathbf{u}(t)$ used to control the AUV.

Stability considerations: The convergence of the proposed observer-feedback control formulation can be assured by studying the error dynamics and using a Lyapunov function argument from [32]. It is possible to locate the eigenvalues of $A_e - K_{e_i} C_e$ in the open left half plane, by modifying the values of the matrix K_{e_i}. Thus, by properly selecting the gains, the dynamics of the prediction errors ($\mathbf{e}_1, \ldots, \mathbf{e}_n$) are globally exponentially stable to 0. This is done by using the argument from the proof of [32, Theorem 4] to select n and K_{e_i} such that the dynamics $\dot{\mathbf{w}}_\star[k] = A_e \mathbf{w}_\star[k] - K_{e_i} C_e \mathbf{w}_\star[t - \tfrac{\tau}{n}]$ with state variable $\mathbf{w}_\star$, are globally exponentially stable to 0 on all of Euclidean space. Note that the system in Equation (24) has a smaller time delay affecting its dynamics, specifically τ/n. Thus, for larger time delays τ, the number of predictors n can be increased, stabilising the system. The only restriction is that $\tau/n \in \mathbb{I}$. If the delay τ is known a priori we could select n to ensure this is always true. Different approaches can be taken to find the parameters in K_{e_i}. In this sense, by locating the eigenvalues of $A_e - K_{e_i} C_e$ in the open left half plane, it will be possible to stabilize the system.

VI. RESULTS

In this section, we present the results obtained using our proposed Koopman-based proportional integrator observer control architecture, which we will refer to as KPIO.

A. EXPERIMENTAL SET-UP

To test the proposed system, we used a modified version of the low-cost Bluerov2 Heavy vehicle that allows for autonomous capabilities [52]. This vehicle has 4-degrees-of-freedom (DOF), which allow for x-, y-, z-, and *yaw*- axis control, and is capable of working at depths of up to 100 m. Since the AUV is controllable in 4-DOF, the pose and velocity vectors are reduced to $\boldsymbol{\eta}(t) = [x_l(t), y_l(t), z_l(t), \psi_a(t)]^T$ and $\boldsymbol{v}(t) = [u(t), v(t), w(t), r(t)]^T$. The vehicle has been modified by incorporating a Water Linked A50 Doppler Velocity Log (DVL) to obtain reliable velocity measurements. The proposed controller is implemented using a robot operating system (or ROS) environment and operates at a frequency of 25 Hz. Experimental data is obtained by deploying the vehicle in a water tank with length × width × depth dimensions of $10 \times 6 \times 3$ m. Position set-point commands and trajectory following are used to evaluate the proposed architecture.

B. SEMI-PARAMETRIC MODELLING EVALUATION

As a direct measurement of the position is unavailable, we utilised the Koopman operator to model the velocity of the AUV, and the pose is obtained by integrating the velocity. Given that the only raw sensor data coming from the vehicle is velocity, we avoided lifting the position component of the state of the system ($\boldsymbol{\eta}$), as this would entail the Koopman operator to be used with data that already has errors coming from another estimation approach, namely by an extended Kalman filter. This resulted in considering the state $\psi(\mathbf{x})$ defined as $\psi(\mathbf{x}) = [\boldsymbol{\eta}, \psi^v(\boldsymbol{v})]^T = [x_l, y_l, z_l, \psi_a, u, v, w, r, \psi_5^v(\boldsymbol{v}), \psi_6^v(\boldsymbol{v})]^T$, where the lifted state $\psi^v(\boldsymbol{v}) = [u, v, w, r, \psi_5^v(\boldsymbol{v}), \psi_6^v(\boldsymbol{v})]^T$, with ψ_5^v and ψ_6^v being randomly distributed Gaussian functions. Therefore, the data pairs to train the Koopman model have the form $\boldsymbol{\alpha}_t = [\psi^v(\boldsymbol{v}(t)), \mathbf{u}(t)]$, and $\boldsymbol{\beta}_t = [\psi^v(\boldsymbol{v}(t + 1)), \mathbf{u}(t)]$. The pairs $\boldsymbol{\alpha}_t$ and $\boldsymbol{\beta}_t$ were obtained by tele-operating the underwater vehicle in random patterns at various velocities. To capture the coupled dynamics of the system, the vehicle has been moved in multiple axes simultaneously. We performed 20 different sets of data collection, each one collecting 4400 data points, of which 3 sets were used for validation. In total, a set of 88,000 data points was obtained at a frequency of 25 Hz, which is less than one hour of motion data. The training was performed on an Intel i7 computer with 16GB of RAM. The same computer was utilised for testing the proposed architecture on the AUV, using ROS.

We compared the obtained Koopman model against a linear model obtained using classical modelling techniques [53], [54]. Figure 2 shows the performance of the developed Koopman model together with the true velocities

TABLE 1. RMSE error comparison for Koopman operator vs classical modelling.

Method	$u(t)$	$v(t)$	$w(t)$	$r(t)$
Koopman	0.0880	0.0601	0.0428	0.3438
Classical	0.1333	0.0870	0.0622	0.6127

and the estimations obtained via the classical model. For this test, the initial state of the Koopman model at time $t = 0$s was set to $\psi^v(\boldsymbol{v}(0))$. We then performed a forward estimation, utilising the true value of the control input and updating the estimated velocities according to Equation (9). We performed the estimation over a long prediction window, starting at $t = 0$s and going to $t = 100$s. As can be seen from Fig. 2a to Fig. 2d, the Koopman model is able to estimate the current velocity of the system with low error. The Koopman model maintains its accuracy even when the prediction window is long. The Koopman model is able to outperform the classical model in every degree of freedom evaluated, a clear difference between the two being seen in Fig. 2d where the classical dynamic modelling presents high spikes and frequencies compared to the actual behaviour of the vehicle.

To further analyse the performance of the Koopman model, we performed 20 tests of 200 seconds each, in which the AUV was commanded to reach a certain position. Similarly as before, the control inputs are fed to both models, and the predicted velocities are recorded. The Root-Mean-Square Error (RMSE) between the predictions and the measured velocities for the 4-DOF is computed, and Table 1 summarises the obtained metrics. It can be seen that the Koopman model presents lower error in every DOF, outperforming the classical model. It can be concluded that the Koopman model performance is accurate, surpassing the performance of other modelling techniques.

C. CONTROL BEHAVIOUR EVALUATION

This section presents the results obtained when using the proposed KPIO methodology. For all experiments in this section, the AUV has a delay in all control inputs equal to $\tau = 2$s. The parameters of the cascaded PID controllers are $K_p^p = diag([0.37, 0.4, 0.15, 0.11])$, $K_i^p = diag([0, 0, 0, 0])$ and $K_d^p = diag([0.1, 0.1, 0.1, 0.1])$ for the position controller, and $K_p^v = diag([9., 9., 7.2, 2.3])$, $K_i^v = diag([0.3, 0.5, 0.01, 0.001])$ and $K_d^v = diag([0.01, 0.01, 0.01, 0.01])$ for the velocity controller. Finally, K_e is composed by matrices K and L (as presented in Section V), with the non-zero elements of K being 8, and the L matrix a diagonal matrix with elements 0.81.

Fig. 3 shows the errors when the desired reference set-point position is $\mathbf{x}_{ref}^p = [4.0 \text{ m}, 0.0 \text{ m}, 0.0 \text{ m}, 0.0 \text{ rad}]^T$. Fig. 3a, shows the error for $x_l(t)$, $y_t(t)$ and $z_l(t)$, where it can be seen how the controller is able to reach the desired position, with a small overshoot in the x axis. Similarly, in Fig. 3b it can be observed how initially there are some oscillation in the yaw
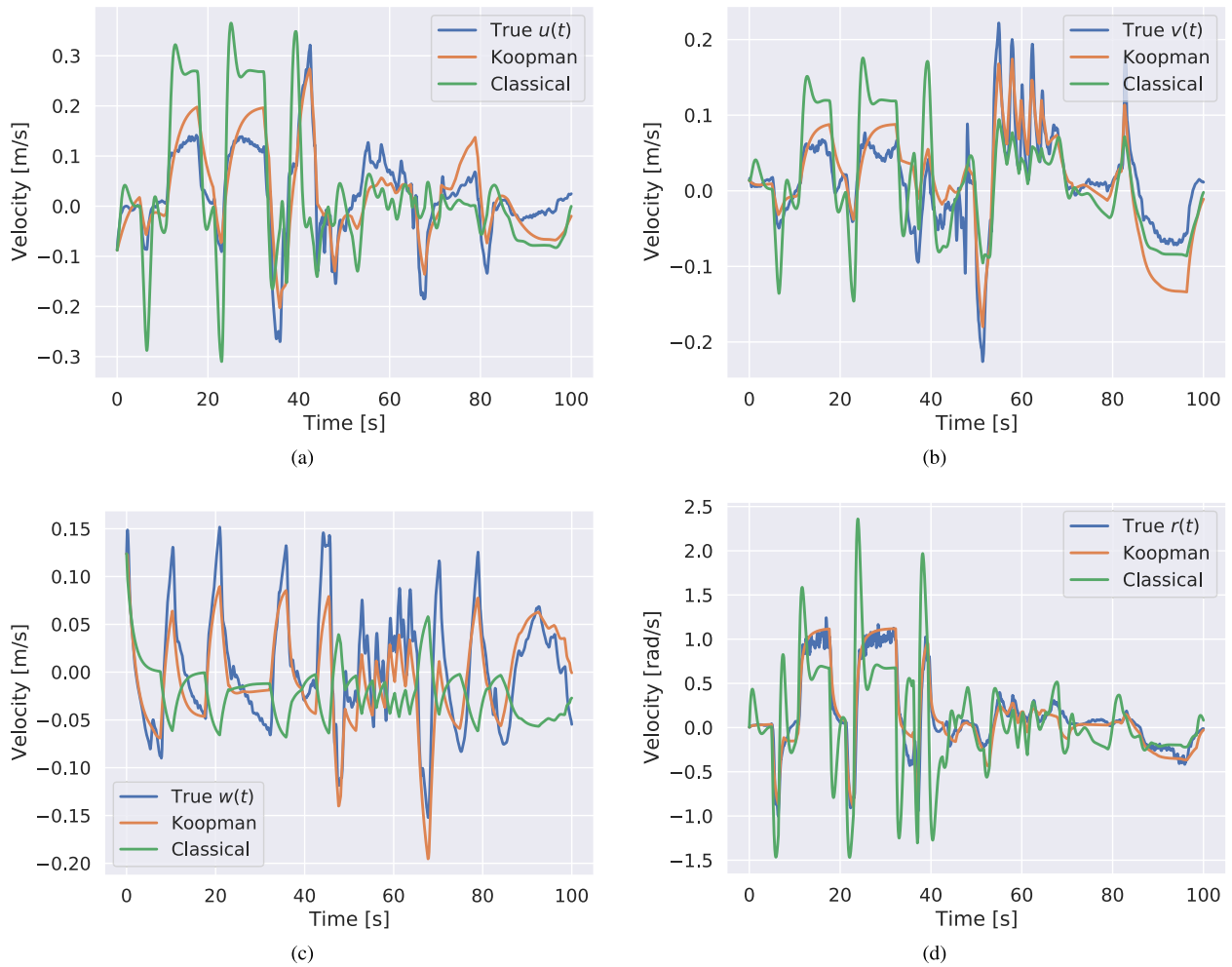
FIGURE 2. The true value of the velocity $v(t) = [u(t), v(t), w(t), r(t)]^T$ versus the Koopman estimation and the linear model obtained with classical modelling techniques. a) Velocity in x axis $u(t)$, b) Velocity in y axis $v(t)$, c) Velocity in z axis $w(t)$, and d) Rotational velocity around z axis $r(t)$.
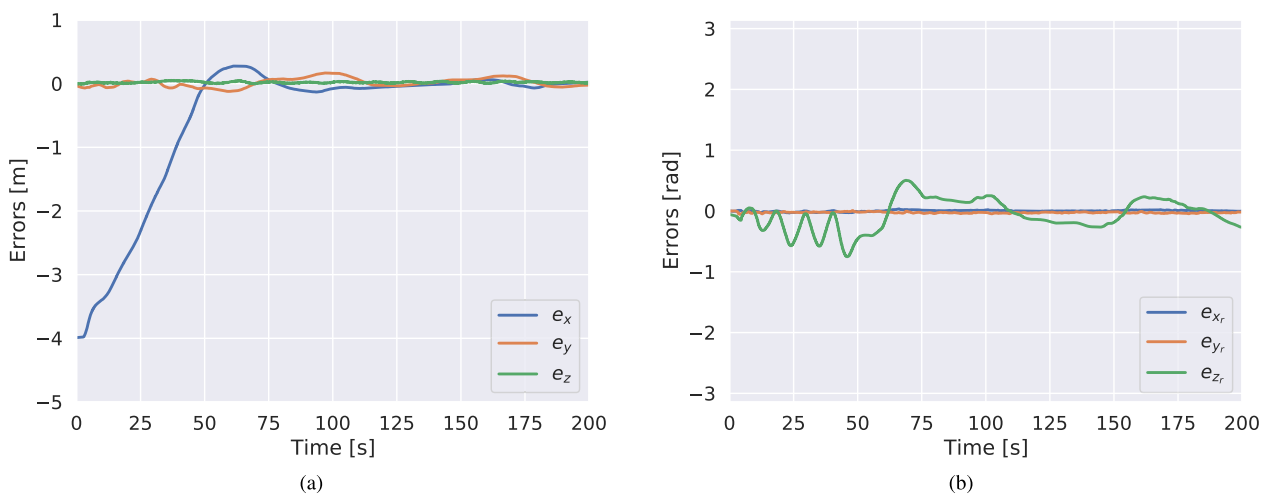

FIGURE 3. Performance of the proposed Koopman Proportional Integral Observer (KPIO) based controller when trying to reach a desired reference point of $x_{ref}^P = [4.0 \text{ m}, \ 0.0 \text{ m}, \ 0.0 \text{ m}, \ 0.0 \text{ rad}]^T$, under a delay of $\tau = 2s$. a) Errors in linear positions; b) Errors in orientation.

that decrease in frequency as time passes. These are caused by the highly coupled dynamics of the AUV. Nevertheless,

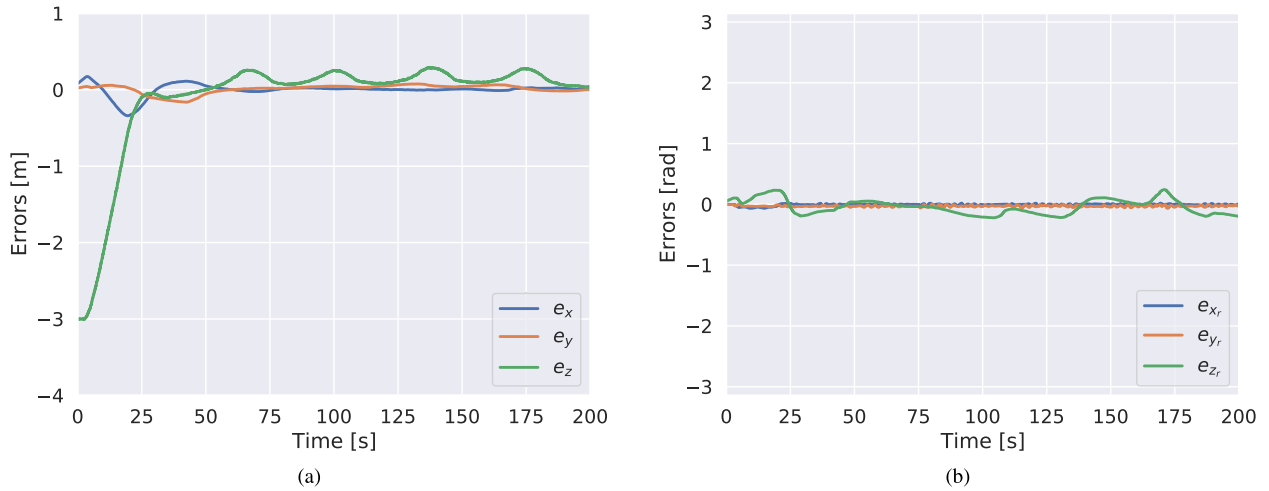the controller is able to achieve and maintain the required position for over 200s. The behaviour of the proposed
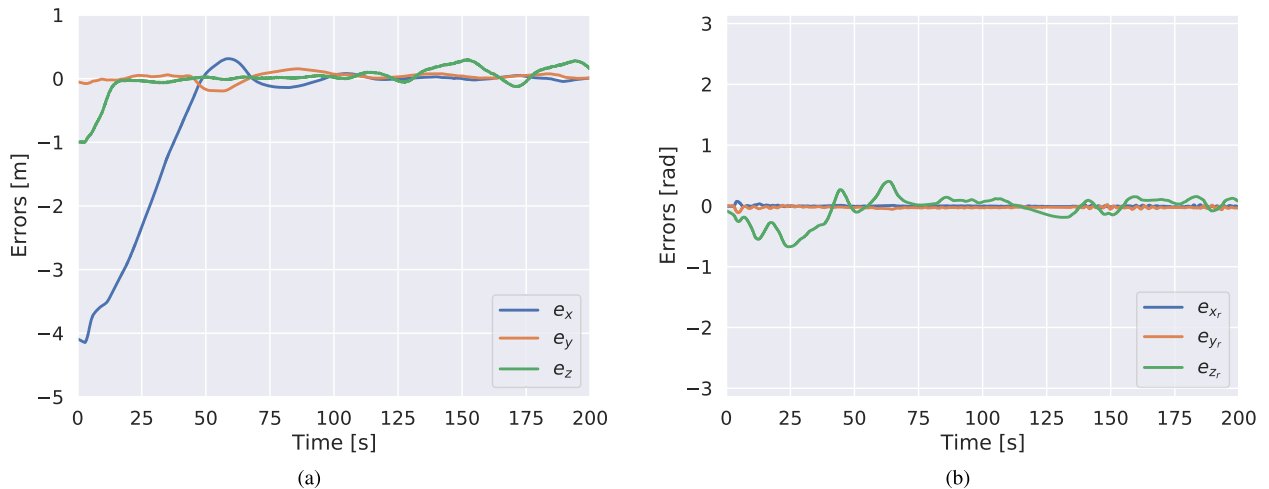
FIGURE 4. Performance of the proposed KPIO based controller when trying to reach a desired reference point of $\mathbf{x}^{p}_{ref} = [0.0 \text{ m}, \ 0.0 \text{ m}, \ 3.0 \text{ m}, \ 0.0 \text{ rad}]^{T}$, under a delay of $\tau = 2s$: a) Errors in linear positions; b) Errors in orientation.

FIGURE 5. Performance of the proposed KPIO based controller when trying to reach a desired reference point of $\mathbf{x}^{p}_{ref} = [4.0 \text{ m}, \ 0.0 \text{ m}, \ 1.0 \text{ m}, \ 0.0 \text{ rad}]^{T}$, under a delay of $\tau = 2s$. a) Errors in linear positions b) Errors in orientation.

methodology is shown in Fig. 4 when a requested depth has to be achieved and maintained. In this case, the requested position is set to $\mathbf{x}^{p}_{ref} = [0.0 \text{ m}, \ 0.0 \text{ m}, \ 3.0 \text{ m}, \ 0.0 \text{ rad}]^{T}$, which means that the AUV has to submerge. The errors in the linear positions are shown in Fig. 4a, where it can be observed that there is no overshoot, however, some oscillations exist once the position has been achieved. In Fig. 4b the yaw presents small variations from the required reference position.

Fig. 5 shows the response of the AUV when different reference goals are requested for several axes at the same time. The vehicle is commanded to achieve the reference defined as $\mathbf{x}^{p}_{ref} = [4.0 \text{ m}, \ 0.0 \text{ m}, \ 1.0 \text{ m}, \ 0.0 \text{ rad}]^{T}$. Fig. 5a shows the error in the linear position when achieving the desired configuration, while Fig. 5b gives the error in the orientation of the vehicle. The AUV is able to achieve the desired reference position with minimal overshoot in under 50 seconds. Similarly, Fig. 6 presents the behaviour of the

AUV when a more complex request task is defined as: $\mathbf{x}^{p}_{ref} = [4.0 \text{ m}, \ 2.5 \text{ m}, \ -2.0 \text{ m}, \ 0.0 \text{ rad}]^{T}$. The errors in position, Fig. 6a, show that the proposed controller is able to achieve the required reference with minimal overshoot and steady-state error. The error in Fig. 6b shows how the yaw $\psi_a(t)$ initially diverges and then later reaches the goal orientation.

To validate the qualitative results presented above, quantitative analysis is performed in which a multitude of different set points are requested. A total of 52 tests are performed where the AUV is commanded to reach various reference points for each axis, both in independent movements and coupled movements (actuation happening at the same time on multiple axes). Several metrics are calculated for each test to quantitatively evaluate the proposed approach. The metrics utilised are: 1) Normalised Root Mean Squared Error (NRMSE), 2) Steady State Error (SSE), 3) Rise Time (RT) in seconds, and 4) Overshoot (OT) in percentage. The average
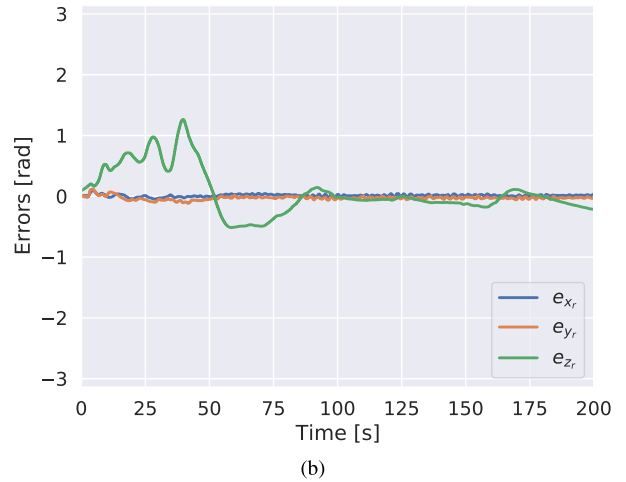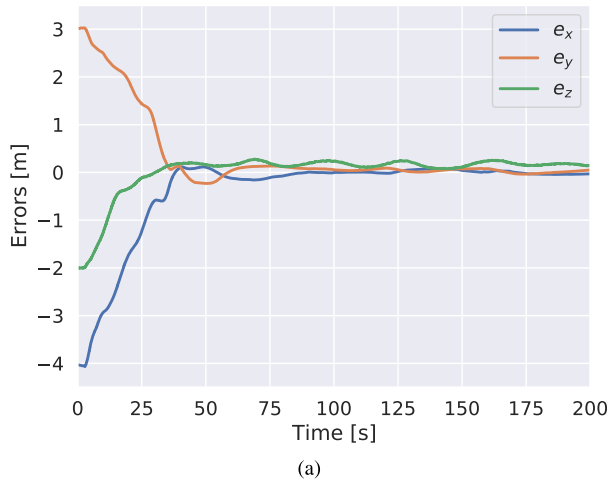
FIGURE 6. Performance of the proposed KPIO based controller when trying to reach a desired reference point of $\mathbf{x}_{ref}^{p}$ = [4.0 m, 2.5 m, −2.0 m, 0.0 rad]^{T}, under a delay of τ = 2s. a) Errors in linear positions b) Errors in orientation.
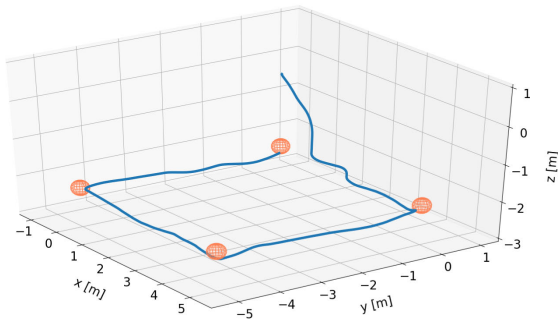

FIGURE 7. Performance of the proposed KPIO based controller when trying to follow a square pattern, under a delay of τ = 2s.

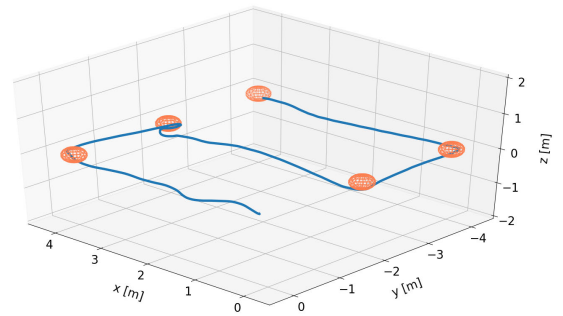**FIGURE 8.** Performance of the proposed KPIO based controller when following a lawnmower pattern, under a delay of τ = 2s.

NRMSE is 0.1856 and the average SSE is 0.0252, showing that the proposed strategy is highly accurate and capable of allowing the AUV to perform station-keeping tasks with high accuracy. The average rising time is RT 13.01 seconds, showcasing that the controller is appropriate for underwater vehicles, which are designed by nature to be slow systems [24]. Finally, the average OT of 9.87% represents a small deviation from the steady state values and these are mostly caused by an underestimation of the real state of the system in the observer formulation.

The proposed KPIO control system is appropriate not only for set-point control but also for trajectory tracking. The results presented in Fig. 7 and Fig. 8 show how the AUV starts in the surface and is requested to follow a predefined trajectory. Fig. 7 shows a square trajectory that the AUV has to follow, ensuring that certain check points are reached (represented by the orange markers). The vehicle, initially has to submerge and reach the operating depth of 2 meters, and after it has to continue to navigate and maintain this depth to reach the checking points. Fig. 8 shows a test where the robot has to follow a lawnmower pattern close to the water's surface.

In both cases, it can be seen that the vehicle successfully reaches the check points, maintaining its operating depth, but due to a slight overshoot in the yaw axis, there are small deviations from achieving a fully straight line.

D. COMPARISON
In this section, we provide a comparison of the proposed KPIO based controller versus the feedback PID without the observer, and a sequential Koopman Proportional Observer (or KPO) controller. The KPO controller utilizes the Koopman model in the sequential prediction, but does not incorporate the integral term in Equation (12) [47].

Fig. 9a shows the error in the linear position, when the desired reference configuration is $\mathbf{x}_{ref}^{p}$ = [1.0 m, 0.0 m, 0.0 m, 0.0 rad]^{T}, while Fig. 9b presents the error in the angular position for the PID controller without the observer. It can be clearly seen how the system rapidly becomes unstable, which forced us to abort the test. In Fig. 10 the behaviour of the robot when a KPO controller is presented. The performance of the system is shown when the same requested configuration is used, that is $\mathbf{x}_{ref}^{p}$ =
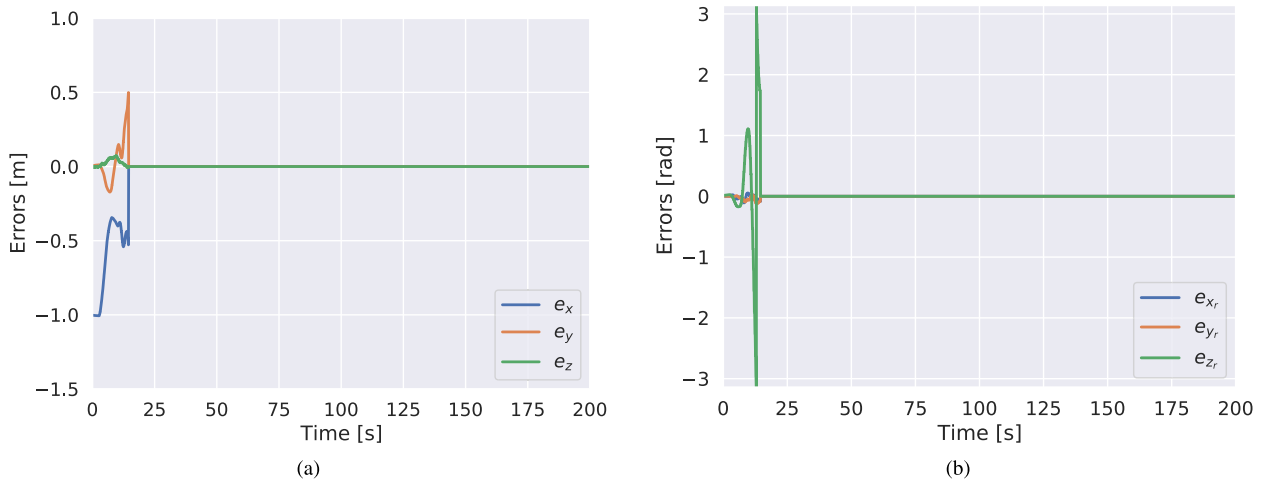
FIGURE 9. Performance of the PID controller when trying to reach a desired reference point of $x_{ref}^P = [1.0\ m,\ 0.0\ m,\ 0.0\ m,\ 0.0\ rad]^T$, under a delay of $\tau = 2s$. a) Errors in linear positions b) Errors in orientation.
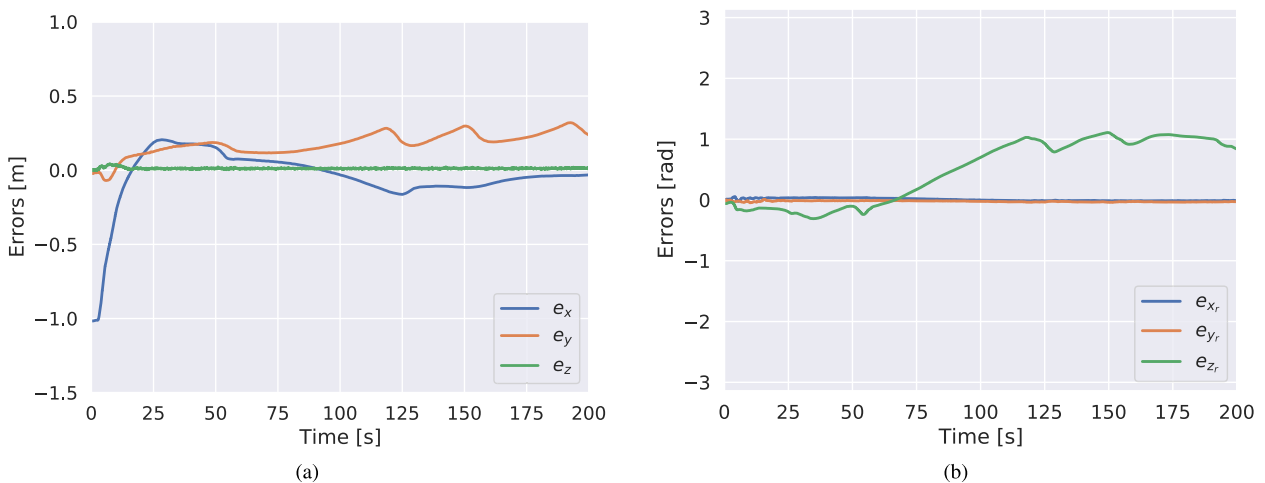

FIGURE 10. Performance of the Koopman Proportional Observer (KPO) controller when trying to reach a desired reference point of $x_{ref}^P = [1.0\ m,\ 0.0\ m,\ 0.0\ m,\ 0.0\ rad]^T$, under a delay of $\tau = 2s$. a) Errors in linear positions b) Errors in orientation.

$[1.0\ m,\ 0.0\ m,\ 0.0\ m,\ 0.0\ m]^T$. Fig. 10a shows the error in the linear positions, while Fig. 10b shows the error in the angular positions. It can be seen that, while the controller drives the AUV towards the requested position, it is unable to maintain the position. High steady-state errors are present with oscillations. Fig. 11 shows the performance when utilising the novel proposed KPIO controller. It can be seen that the controller is able to reach the desired position, with low errors as observed in Fig. 11a and Fig. 11b. Additionally, while rise time values are similar for both KPIO and KPO, the proposed KPIO controller is able to reach the desired position faster and to maintain it.

Table 2 presents the quantitative evaluation of the above mentioned control algorithms for 4 tests. These tests require the vehicle to move to various reference goals, actuating both the linear and angular DOFs of the vehicle. Similarly as before, a delay of 2 seconds is used. In the table, a dash "−" indicates that the task was not successfully solved by

the corresponding algorithm. The proposed KPIO controller outperforms the other methods, being able to successfully achieve the required tasks, while at the same time having smaller errors and oscillations compared to the KPO. Particularly, our method provides a 40% improvement in NRMSE performance, when compared with the KPO for the successful cases. The PID is unable to complete most of the tasks, except Task 2. In this task, the reference was set to $x_{ref}^p = [0.0\ m,\ 0.0\ m,\ 2.0\ m,\ 0.0\ m]^T$ and due to the decoupled dynamics of the z axis, it represents a simpler problem that the PID is able to solve, although with high values of overshoot and rise time.

E. DISCUSSION
The nonlinear dynamics of the AUV in combination with the delayed inputs result in a system that is difficult to control. Nevertheless, the proposed KPIO approach was able to obtain successful results. One of the main advantages of the pro-
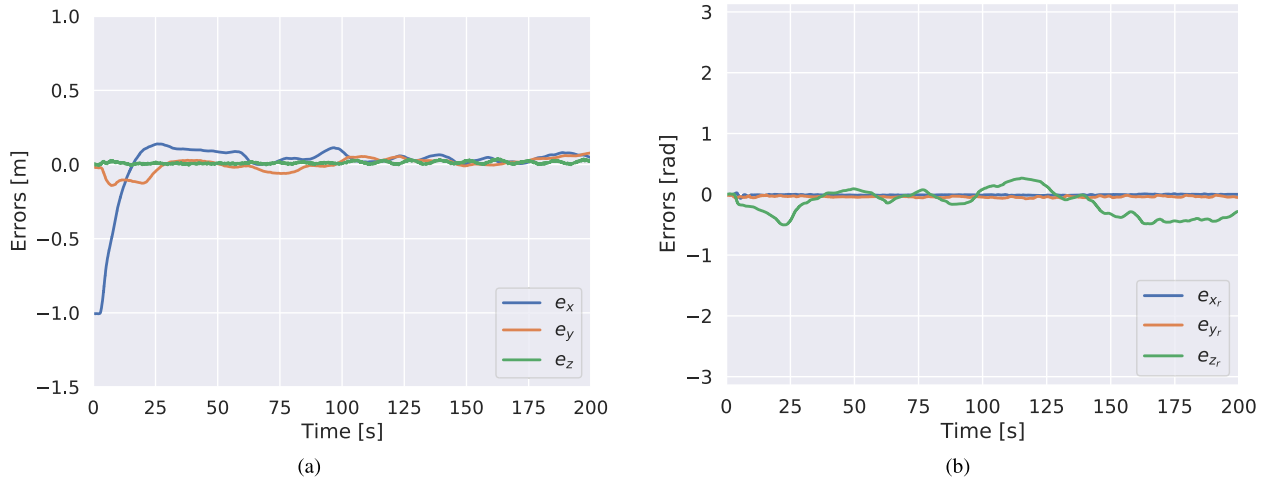
FIGURE 11. Performance of the proposed KPIO controller when trying to reach a desired reference point of $x_{ref}^p = [1.0 \text{ m}, \ 0.0 \text{ m}, \ 0.0 \text{ m}, \ 0.0 \text{ m}]^T$, under a delay of $\tau = 2s$. a) Errors in linear positions b) Errors in orientation.

TABLE 2. Performance comparison of the proposed algorithm for different tasks.

Task	Type	NRMSE	SSE	RT [s]	OS[%]
1	KPIO	0.1254	0.02192	13.24	8.79
	KPO	0.2802	0.19005	13.32	23.88
	PID	-	-	-	-
2	KPIO	0.1526	0.02211	15.84	1.92
	KPO	-	-	-	-
	PID	0.1099	0.00814	19.16	11.54
3	KPIO	0.2421	0.00299	32.16	6.25
	KPO	0.2597	0.07684	34.25	8.75
	PID	-	-	-	-
4	KPIO	0.1056	0.003466	5.101	20.36
	KPO	0.2519	0.06624	11.19	39.12
	PID	-	-	-	-

posed methodology relies on the data-driven characteristics of the control system. The Koopman operator provides a simple and fast methodology for obtaining a linear model of the AUV, offering excellent performance while at the same time maintaining a low computational cost, crucial in low-cost autonomous vehicles. Furthermore, this data-driven approach results in a semi-parametric description of the system that combines an equation-based representation with a data-driven parameter estimation. However, while our Koopman model provides good performance, the method is not limited to the use of a Koopman based model. In fact, the predictor-based control architecture can use any linear model of the vehicle. This is an advantage, especially in systems in which accurate linear models can be computed with methods such as Newton-Euler or Euler-Lagrange. The proposed observer provides a simple implementation in matrix form, which allows for fast computation of the future state. Furthermore, the sequential characteristic of the observer makes the effect of the delay on each subsystem smaller, by subdividing for the number of predictors, relaxing the selection of the gains and allowing it to work with longer delays.

One of the main concerns when working with model-based methods is obtaining a model that is able to accurately represent the behaviour of the vehicle. Initial experiments done with a linearised model of the AUV obtained with traditional modelling techniques [54] showed significant differences between the actual behaviour of the AUV and the predictions obtained with the model, which hindered the performance of the observer. While the model obtained by means of the Koopman operator improved the performance, there are still some challenges, particularly with regard to angular velocity, that require further investigation. Affordable sensors, like those on board the low-cost underwater vehicle used for our trials [52], might not be sufficient for providing an accurate model representation, and therefore higher quality Inertial Measurement Units (or IMUs) may be required [55], [56]. Another characteristic of the proposed approach is that the obtained model is pre-trained and then fixed during execution, meaning that any subsequent data obtained is not utilised to improve the model. A real-time adaptation mechanism could be considered, in which real-time data is utilised to improve the model. Future improvements of the Koopman modelling technique could be considered to include an additional term that accounts for disturbances in the system, leading to a simplified observer representation. Additionally, while the controller is able to stabilise the system, further work is needed to investigate this in detail, particularly for cases in which hard position constraints are required. Future work can also investigate how other types of controllers, such as fixed-time controllers [28], can be integrated with the Koopman-based sequential predictors.

VII. CONCLUSION

In this article, we introduced a novel control architecture for AUVs working under communication delays. We based the proposed approach on the predictor based theory, which is expanded here to incorporate highly nonlinear complex

systems, such as marine vehicles. The observer predictor formulation was leveraged to obtain a feedback control law that is able to compensate for uncertainties in the state caused by delays in the communication channels of the robot. Furthermore, a data-driven model was incorporated, based on Koopman operator theory, that can replace classical dynamic models, while at the same time providing a semi-parametric approximation that can be readily incorporated into linear control formulations.

A real-time evaluation of our proposed control strategy was performed on a low-cost underwater vehicle under the influence of time delays. The obtained results show that our control formulation is able to successfully reach stable behaviour, even in the presence of long delays. A comparative analysis with a simple PID approach shows that under such uncertainty, the PID is unable to reach the desired reference.

In future work, the present formulation will be applied to higher degree-of-freedom platforms such as an underwater vehicle manipulator system (or UVMS). Furthermore, the Koopman operator will be used to accurately incorporate disturbances in the system.

REFERENCES

[1] R. O'Rourke, *Navy Large Unmanned Surface and Undersea Vehicles: Background and Issues for Congress*. Washington, DC, USA: Congressional Research Service, 2019.

[2] M. Ludvigsen, F. Søreide, K. Aasly, S. Ellefmo, M. Zylstra, and M. Pardey, "ROV based drilling for deep sea mining exploration," in *Proc. OCEANS*, Jun. 2017, pp. 1–6.

[3] M. Montseny, C. Linares, N. Viladrich, M. Biel, N. Gracias, P. Baena, E. Quintanilla, S. Ambroso, J. Grinyó, A. Santín, J. Salazar, M. Carreras, N. Palomeras, L. Magí, G. Vallicrosa, J.-M. Gili, and A. Gori, "Involving fishers in scaling up the restoration of cold-water coral gardens on the Mediterranean continental shelf," *Biol. Conservation*, vol. 262, Feb. 2021, Art. no. 109301.

[4] Y. Wang, S. Jiang, B. Chen, and H. Wu, "Trajectory tracking control of underwater vehicle-manipulator system using discrete time delay estimation," *IEEE Access*, vol. 5, pp. 7435–7443, 2017.

[5] V. M. Hung and U. J. Na, "Remote control system of a 6 DOF underwater robot," in *Proc. Int. Conf. Control, Autom. Syst.*, Oct. 2008, pp. 2575–2580.

[6] M. S. Triantafyllou and M. A. Grosenbaugh, "Robust control for underwater vehicle systems with time delays," *IEEE J. Ocean. Eng.*, vol. 16, no. 1, pp. 146–151, Jun. 1991.

[7] P. Farajiparvar, H. Ying, and A. Pandya, "A brief survey of telerobotic time delay mitigation," *Frontiers Robot. AI*, vol. 7, p. 198, Dec. 2020.

[8] J. Yuh, "Design and control of autonomous underwater robots: A survey," *Auton. Robots*, vol. 8, no. 1, pp. 7–24, 2000.

[9] R. P. Kumar, A. Dasgupta, and C. Kumar, "Robust tracking control of underwater vehicles using time-delay control in discrete-time domain," in *Proc. OCEANS*, Jun. 2006, pp. 1–5.

[10] K. Liu, G. Xu, Q. Yang, and Z. Zhao, "Optimal disturbance suppression of disturbed underwater vehicle with state delay," *IEEE Access*, vol. 10, pp. 63984–63990, 2022.

[11] I. Bhogaraju, M. Farasat, M. Malisoff, and M. Krstic, "Sequential predictors for delay-compensating feedback stabilization of bilinear systems with uncertainties," *Syst. Control Lett.*, vol. 152, Jun. 2021, Art. no. 104933.

[12] E. Sontag, "Input to state stability: Basic concepts and results," in *Nonlinear and Optimal Control Theory*, P. Nistri and G. Stefani, Eds. Berlin, Germany: Springer, 2008, pp. 163–220.

[13] F. Mazenc, M. Malisoff, and I. N. S. Bhogaraju, "Sequential predictors for delay compensation for discrete time systems with time-varying delays," *Automatica*, vol. 122, Dec. 2020, Art. no. 109188.

[14] I. Carlucho, D. W. Stephens, and C. Barbalata, "An adaptive data-driven controller for underwater manipulators with variable payload," *Appl. Ocean Res.*, vol. 113, Aug. 2021, Art. no. 102726.

[15] D. Ha and J. Schmidhuber, "Recurrent world models facilitate policy evolution," in *Proc. Adv. Neural Inf. Process. Syst.*, S. Bengio, H. Wallach, H. Larochelle, K. Grauman, N. Cesa-Bianchi, and R. Garnett, Eds. Red Hook, NY, USA: Curran Associates, 2018, pp. 2450–2462.

[16] M. O. Williams, I. G. Kevrekidis, and C. W. Rowley, "A data–driven approximation of the Koopman operator: Extending dynamic mode decomposition," *J. Nonlinear Sci.*, vol. 25, no. 6, pp. 1307–1346, Dec. 2015.

[17] C. Folkestad, Y. Chen, A. D. Ames, and J. W. Burdick, "Data-driven safety-critical control: Synthesizing control barrier functions with Koopman operators," *IEEE Control Syst. Lett.*, vol. 5, no. 6, pp. 2012–2017, Dec. 2021.

[18] E. Kaiser, J. N. Kutz, and S. L. Brunton, "Data-driven discovery of Koopman eigenfunctions for control," *Mach. Learn., Sci. Technol.*, vol. 2, no. 3, Jun. 2021, Art. no. 035023.

[19] D. Bruder, X. Fu, R. B. Gillespie, C. D. Remy, and R. Vasudevan, "Data-driven control of soft robots using Koopman operator theory," *IEEE Trans. Robot.*, vol. 37, no. 3, pp. 948–961, Jun. 2021.

[20] M. Korda and I. Mezic, "Koopman model predictive control of nonlinear dynamical systems," in *The Koopman Operator in Systems and Control* (Lecture Notes in Control and Information Sciences), vol. 484. Springer, 2020, pp. 235–255.

[21] S. Zhao and J. Yuh, "Experimental study on advanced underwater robot control," *IEEE Trans. Robot.*, vol. 21, no. 4, pp. 695–703, Aug. 2005.

[22] I. Carlucho, M. De Paula, S. Wang, Y. Petillot, and G. G. Acosta, "Adaptive low-level control of autonomous underwater vehicles using deep reinforcement learning," *Robot. Auto. Syst.*, vol. 107, pp. 71–86, Sep. 2018.

[23] L. Shi, S. Su, S. Guo, K. Tang, S. Pan, Y. He, H. Xing, Z. Chen, and P. Guo, "A fuzzy PID control method for the underwater spherical robot," in *Proc. IEEE Int. Conf. Mechatronics Autom. (ICMA)*, Aug. 2017, pp. 626–631.

[24] C. Barbelate, V. De Carolis, M. W. Dunnigan, Y. Pétillot, and D. Lane, "An adaptive controller for autonomous underwater vehicles," in *Proc. IEEE/RSJ Int. Conf. Intell. Robots Syst. (IROS)*, Sep. 2015, pp. 1658–1663.

[25] J. Xu and C. Yang, "An improved time delay controller for underwater robot," in *Proc. IEEE Int. Conf. Robot. Biomimetics*, Dec. 2011, pp. 2307–2311.

[26] C. Suryendu and B. Subudhi, "Formation control of multiple autonomous underwater vehicles under communication delays," *IEEE Trans. Circuits Syst. II, Exp. Briefs*, vol. 67, no. 12, pp. 3182–3186, Dec. 2020.

[27] L. Zhao, H. Ma, L. Xu, and X. Wang, "Observer-based adaptive sampled-data event-triggered distributed control for multi-agent systems," *IEEE Trans. Circuits Syst. II, Exp. Briefs*, vol. 67, no. 1, pp. 97–101, Jan. 2020.

[28] Y. Liu, H. Li, R. Lu, Z. Zuo, and X. Li, "An overview of finite/fixed-time control and its application in engineering systems," *IEEE/CAA J. Autom. Sinica*, vol. 9, pp. 2106–2120, 2022.

[29] Z. Gao and G. Guo, "Fixed-time sliding mode formation control of AUVs based on a disturbance observer," *IEEE/CAA J. Autom. Sinica*, vol. 7, no. 2, pp. 539–545, Jun. 2020.

[30] E. Morgan, I. Carlucho, W. Ard, and C. Barbalata, "Autonomous underwater manipulation: Current trends in dynamics, control, planning, perception, and future directions," *Current Robot. Rep.*, vol. 3, no. 4, pp. 187–198, Jul. 2022.

[31] J. Weston and M. Malisoff, "Sequential predictors under time-varying feedback and measurement delays and sampling," *IEEE Trans. Autom. Control*, vol. 64, no. 7, pp. 2991–2996, Jul. 2019.

[32] G. Besançon, D. Georges, and Z. Benayache, "Asymptotic state prediction for continuous-time systems with delayed input and application to control," in *Proc. Eur. Control Conf. (ECC)*, Jul. 2007, pp. 1786–1791.

[33] M. Najafi, S. Hosseinnia, F. Sheikholeslam, and M. Karimadini, "Closed-loop control of dead time systems via sequential sub-predictors," *Int. J. Control*, vol. 86, no. 4, pp. 599–609, Apr. 2013.

[34] M. Najafi, F. Sheikholeslam, Q. Wang, and S. Hosseinnia, "Robust H_∞ control of single input-delay systems based on sequential sub-predictors," *IET Control Theory Appl.*, vol. 8, no. 13, pp. 1175–1184, Sep. 2014.

[35] M. H. Khodayari and S. Balochian, "Modeling and control of autonomous underwater vehicle (AUV) in heading and depth attitude via self-adaptive fuzzy PID controller," *J. Mar. Sci. Technol.*, vol. 20, no. 3, pp. 559–578, Sep. 2015.

[36] I. Carlucho, B. Menna, M. De Paula, and G. G. Acosta, "Comparison of a PID controller versus a LQG controller for an autonomous underwater vehicle," in *Proc. 3rd IEEE/OES South Amer. Int. Symp. Ocean. Eng. (SAISOE)*, Jun. 2016, pp. 1–6.

[37] K. M. Bossley, M. Brown, and C. J. Harris, "Neurofuzzy identification of an autonomous underwater vehicle," *Int. J. Syst. Sci.*, vol. 30, no. 9, pp. 901–913, Jan. 1999.

[38] X. Qin, W. Zhang, S. Gao, X. He, and J. Lu, "Sensor fault diagnosis of autonomous underwater vehicle based on LSTM," in *Proc. 37th Chin. Control Conf. (CCC)*, Jul. 2018, pp. 6067–6072.

[39] B. Lusch, J. N. Kutz, and S. L. Brunton, "Deep learning for universal linear embeddings of nonlinear dynamics," *Nature Commun.*, vol. 9, no. 1, p. 4950, Nov. 2018.

[40] Y. Li, H. He, J. Wu, D. Katabi, and A. Torralba, "Learning compositional Koopman operators for model-based control," in *Proc. 8th Int. Conf. Learn. Represent. (ICLR)*, Addis Ababa, Ethiopia, Apr. 2020, pp. 1–14.

[41] M. Budišić, R. Mohr, and I. Mezić, "Applied koopmanism," *Chaos, Interdiscipl. J. Nonlinear Sci.*, vol. 22, no. 4, Dec. 2012, Art. no. 047510.

[42] M. Korda and I. Mezić, "Linear predictors for nonlinear dynamical systems: Koopman operator meets model predictive control," *Automatica*, vol. 93, pp. 149–160, Jul. 2018.

[43] Z. Chen, Z. Lin, X. Zhai, and J. Liu, "Dynamic wind turbine wake reconstruction: A Koopman-linear flow estimator," *Energy*, vol. 238, Jan. 2022, Art. no. 121723.

[44] J. Wang and O. R. Barry, "Exploring data-driven modeling and analysis of nonlinear pathological tremors," *Mech. Syst. Signal Process.*, vol. 156, Jul. 2021, Art. no. 107659.

[45] Q. Li, F. Dietrich, E. M. Bollt, and I. G. Kevrekidis, "Extended dynamic mode decomposition with dictionary learning: A data-driven adaptive spectral decomposition of the Koopman operator," *Chaos, Interdiscipl. J. Nonlinear Sci.*, vol. 27, no. 10, Oct. 2017, Art. no. 103111.

[46] A. Radke and Z. Gao, "A survey of state and disturbance observers for practitioners," in *Proc. Amer. Control Conf.*, 2006, pp. 1–6.

[47] F. Bakhshande and D. Söffker, "Proportional-integral-observer: A brief survey with special attention to the actual methods using ACC benchmark," *IFAC-PapersOnLine*, vol. 48, no. 1, pp. 532–537, Jan. 2015.

[48] J. Xu, C. C. Mi, B. Cao, J. Deng, Z. Chen, and S. Li, "The state of charge estimation of lithium-ion batteries based on a proportional-integral observer," *IEEE Trans. Veh. Technol.*, vol. 63, no. 4, pp. 1614–1621, May 2014.

[49] F. Mazenc, M. Malisoff, and Z. Lin, "Further results on input-to-state stability for nonlinear systems with delayed feedbacks," *Automatica*, vol. 44, no. 9, pp. 2415–2421, Sep. 2008.

[50] M. M. Hammad, A. K. Elshenawy, and M. I. El Singaby, "Position control and stabilization of fully actuated AUV using PID controller," in *Proc. SAI Intell. Syst. Conf. (IntelliSys)*, Y. Bi, S. Kapoor, and R. Bhatia, Eds. Cham, Switzerland: Springer, 2018, pp. 517–536.

[51] W. Bolton, "13—Controllers," in *Instrumentation and Control Systems*, W. Bolton, Ed. Oxford, U.K.: Newnes, 2004, pp. 290–302.

[52] J. S. Willners, I. Carlucho, S. Katagiri, C. Lemoine, J. Roe, D. Stephens, T. Luczynski, S. Xu, Y. Carreno, È. Pairet, C. Barbalata, Y. Petillot, and S. Wang, "From market-ready ROVs to low-cost AUVs," in *Proc. OCEANS*, Sep. 2021, pp. 1–7.

[53] C.-J. Wu, "6-DoF modelling and control of a remotely operated vehicle," M.S. thesis, College Sci. Eng., Flinders Univ., Bedford Park, SA, Australia, 2018.

[54] T. Fossen, *Guidance and Control of Ocean Vehicles*. New York, NY, USA: Wiley, 1994.

[55] P. D. Groves, "Navigation using inertial sensors [tutorial]," *IEEE Aerosp. Electron. Syst. Mag.*, vol. 30, no. 2, pp. 42–69, Feb. 2015.

[56] J. H. Kepper, B. C. Claus, and J. C. Kinsey, "A navigation solution using a MEMS IMU, model-based dead-reckoning, and one-way-travel-time acoustic range measurements for autonomous underwater vehicles," *IEEE J. Ocean. Eng.*, vol. 44, no. 3, pp. 664–682, Jul. 2019.

IGNACIO CARLUCHO (Member, IEEE) received the B.S. degree in electromechanical engineering and the Ph.D. degree in engineering from National Buenos Aires Province Centre University, Argentina, in 2015 and 2019, respectively. From 2020 to 2021, he was a Postdoctoral Researcher with the Department of Mechanical and Industrial Engineering, Louisiana State University, and from 2021 to 2023, he was a Postdoctoral Researcher with the School of Informatics, The University of Edinburgh, U.K. He is currently an Assistant Professor with Heriot-Watt University. His research interest includes intelligent control techniques for marine robotics.

DYLAN STEPHENS received the B.S. degree in mechanical engineering from Louisiana State University, in 2020. He is currently an Autonomous Vehicle Engineer with Einride. His research focuses on developing control systems for underwater manipulators and ROVs. His research interests include robotics, nonlinear control, and the modeling of dynamical systems.

WILLIAM ARD received the bachelor's degree in mechanical engineering with a minor in robotics from Louisiana State University (LSU), where he is currently pursuing the Graduate degree with the Department of Mechanical and Industrial Engineering. He is a member of the Innovation in Control and Robotics Engineering Laboratory (iCORE Laboratory), where he studies motion planning and computer vision in the domain of industrial and underwater robotics.

CORINA BARBALATA received the B.S. degree in electrical engineering from Transilvania University, Romania, in 2011, the double M.S. degree in computer vision and robotics from Heriot-Watt University, Scotland, U.K., and University of Burgundy, France, in 2013, through the VIBOT Program, and the Ph.D. degree in electrical engineering from Heriot-Watt University, in 2017. From 2017 to 2019, she was a Postdoctoral Researcher with the Naval Architecture and Marine Engineering Department, University of Michigan. She is currently an Assistant Professor with the Mechanical Engineering Department, Louisiana State University.

● ● ●